PAPER U

CROSSWELL SEISMIC IMAGING IN THE PERMIAN BASIN: TWO CASE HISTORIES

R. T. Langan, J. M. Harris, S. K. Lazaratos, and T. L. Jensen‡

ABSTRACT

Crosswell seismic imaging technology has advanced rapidly over the last three years as the processing methods have become more robust, the cost of data acquisition has fallen, and the interwell distances of operation have increased. The Permian Basin of West Texas is proving to be an ideal environment in which to develop this technology because of the relatively low seismic attenuation of the carbonate-dominated lithology, the moderate well spacings in the large number of mature fields, and the unusually high number of reflecting horizons. Current technology permits us to operate in carbonates at well spacings on the order of 2000 ft (650 m) and to image *P*- and *S*-wave reflecting horizons on a scale of 8 to 25 ft (2.4 to 7.6 m). Crosswell technology is not limited to carbonates, although the majority of recent applications have been in this environment.

In this paper we discuss two different crosswell experiments in the Permian Basin, each with unique objectives. The first experiment deals with a waterflood in a Middle Clearfork Formation reservoir on the Eastern Shelf, where we are trying to explain the erratic response of adjacent wells to water injection. In the second project we are trying to image the structure and stratigraphy associated with subtle "anomalies" in 3-D surface seismic images of the Wolfcamp Formation. Figure 1 shows the general location of the Midland Basin (where the lithologies are presumably consistent with deeper water) and the Eastern Shelf, relative to the location of the well-known Grayburg Formation reservoirs (e.g., McElroy) of the Central Basin Platform.

INTRODUCTION

Two recent innovations have had a major impact on crosswell seismic technology. The first is the acquisition method of "shooting on the fly". In this method the downhole source is fired at preset depth intervals as it moves continuously up the borehole, while the receivers are fixed in position (Harris et al., 1995). This technique permits an acquisition rate of more than 20,000 seismic traces in one day, which results in sharply reduced costs and minimizes the disruption of field operations.

The second innovation is the implementation of a true interwell reflection imaging algorithm for real data (Lazaratos et al., 1995) capable of imaging reflectors from one well to the other. This algorithm is a variant of methods used to image offset VSP's, except the number of traces in our crosswell data sets is many times greater than those collected with offset VSP's.

We have been pursuing a variety of applications in the mature oil fields of the Permian Basin in West Texas in order to drive the development of the technology. The Permian Basin provides an environment that has made it easier to overcome many prior problems associated with data acquisition and processing. For example, even though our source is of

----

‡Chevron USA, Midland, Texas

relatively low power, the transmissive carbonates (high Q) of this region combined with the relatively close well spacings permit the collection of high signal-to-noise ratio data. Secondly, the high P- and S-wave velocities of these carbonates relative to water velocity make it possible to separate the components of the reflected wavefield from coherent noise associated with tube waves. Finally, the highly variable velocity and density structure of these carbonates gives rise to wavefields rich in reflected energy, which has been helpful in developing imaging algorithms suitable for crosswell geometries.

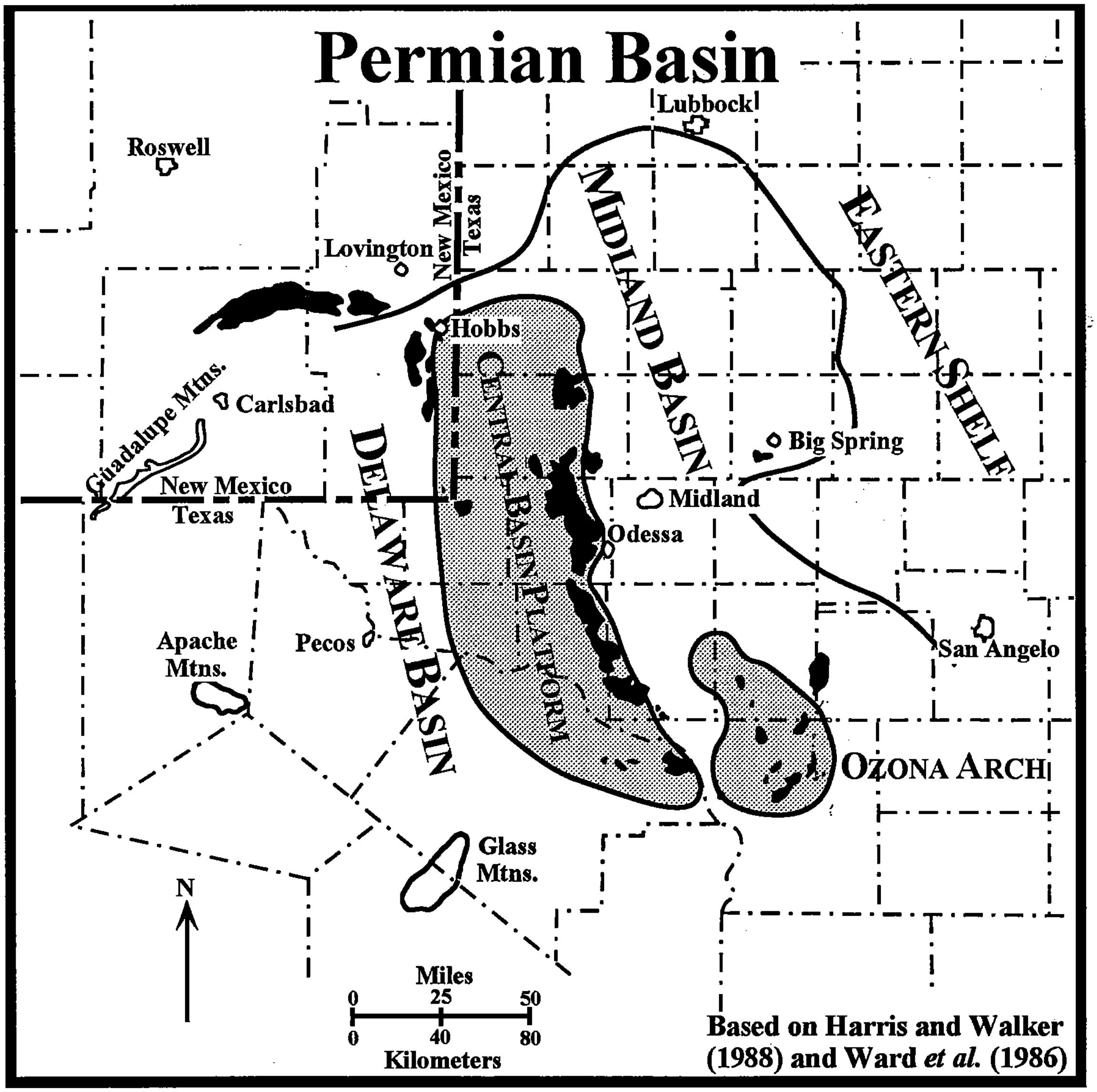

Figure 1. The main paleogeographic provinces of the Permian Basin of West Texas are outlined in relation to major oil fields producing from the Grayburg Formation (black regions).

The geophysical conditions in the Permian Basin are not the only reason for developing the technology in this location. The large reserves still remaining in many of the mature oil fields require increasingly sophisticated techniques to extract. These techniques may be more effectively designed and implemented using information available from crosswell seismic technology.

The two case histories summarized in this paper are still active research projects. We have provided interpretations, some speculative, based upon the crosswell images in order to demonstrate the potential of their unusually high resolution. This resolution is possible because the data were collected using a relatively high frequency source (the piezoelectric element was swept in frequency from 200 Hz to 2000 Hz in most cases) and a closely spaced, five-level hydrophone string.

CASE STUDY I: WATERFLOOD PROJECT

Our first example is from a waterflood project in an oil field on the western edge of the Eastern Shelf (see Figure 1). The reservoir is a 300-ft-thick (91 m) interval in the Middle Clearfork Formation, also a carbonate. The injection rates are unpredictable from one well to the next, which is difficult to explain from the information available from the well logs. The 3-D surface seismic data suggest a slight westward dip of the strata towards the Midland Basin, but the seismic resolution is on the order of the half-thickness of the producing interval itself. We collected three crosswell profiles between four water injectors as shown in Figure 2. We chose this layout in order to obtain a 3-D perspective around a well that was not accepting water. The average injection rate for water at each well is shown in gallons per day (1 gallon = 3.785 liters).

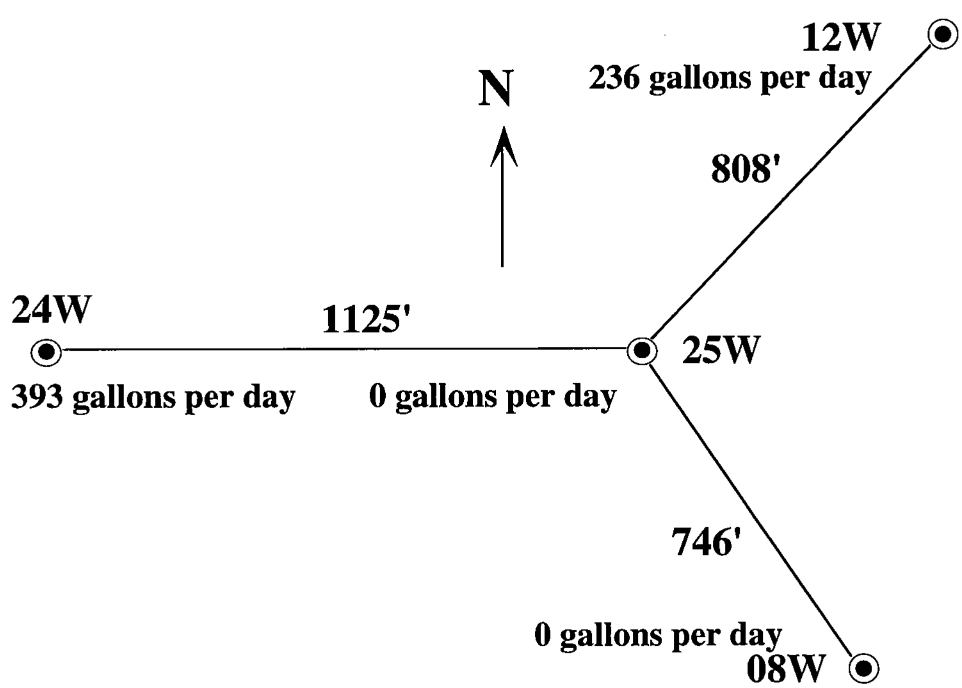

Figure 2. An outline of the three crosswell profiles which tie together four water injectors in our waterflood study.

The reflection images for two of the profiles are shown in Figure 3. These two profiles are nearly orthogonal, but give a dominantly north-south regional perspective. The top of the reservoir is at a depth of about 2840 ft and is characterized by thin laminations. The characteristic wavelength in this zone is on the order of 15 ft (4.6 m).

At these well spacings, 752 ft (229 m) and 802 ft (244 m), the energy propagation distances are at the upper limit of what was detectable for the tools available when we collected these data in late 1993. This results in the poor signal-to-noise ratio seen in the center of the sections, and elsewhere.

These reflection images suggest there may be some eastwardly dipping faults near injector Well 25W with displacements on the order of 10 ft (3.0 m). These faults could disrupt flow in various horizons, which might explain why this well will not take water. Some of these interpreted faults are indicated by the white lines superposed on the section. There is difficulty in tying the faults at the well, which may be in part due to our current processing methods--reflections within a few feet of the source and receiver wells are unintentionally removed by filters used to remove the transmitted arrivals. Another explanation is that we have "over-interpreted" the image. The true dip of these faults is probably greater than the apparent dip on each section. Both lines appear to be oblique to the dip of the fault planes.

There also appears to be a westwardly dip on the order of 1° in many of the reflecting horizons and there is a hint of several stratigraphic pinchouts. These features may also affect the waterflood response.

Figure 4 shows the reflection image from the remaining profile, but it is of poorer quality because of the greater propagation distances involved. However, one can see a slight westwardly dip of many strata and the presence of pinchouts in this section. The frequency content of the reflections is lower and the noise level is greater. The resolution is such that we are unable to see the continuation of the faults interpreted in Figure 3. However, improved wavefield separation and mapping methods developed since these data were processed may improve the image if it is reprocessed.

CASE STUDY II: IMAGING AN "ANOMALY"

Modern 3-D surface seismic data collected in the Midland Basin have revealed subtle amplitude anomalies in the carbonate-rich Wolfcamp Formation. These anomalies are at the threshold of seismic resolution and sometimes contain reservoir-quality carbonates. Information from wells that either penetrate or narrowly miss these anomalies gives only a partial explanation. One well which penetrated an "anomaly" encountered a massive limestone unit, while a nearby well encountered siliciclastic-rich carbonates at the same depth, which one could interpret as debris. Of interest is the internal structure of these "anomalies", their stratigraphic relationship with adjacent strata, and the depositional environment. An opportunity to address these questions with a crosswell survey occurred because there were two wells available for study, one that had penetrated the anomaly, the other which missed, and they were separated by only about 640 ft (195 m).

Some of the operational aspects of this survey are still proprietary, but we can discuss the imaging results and their interpretation in a general sense.

A velocity tomogram computed from the transmitted energy is presented in Figure 5a. It was constructed using the adaptive-gridding technique of Harris (1994). The basis of this algorithm is the definition of velocity through the use of a sparse grid of nodes.

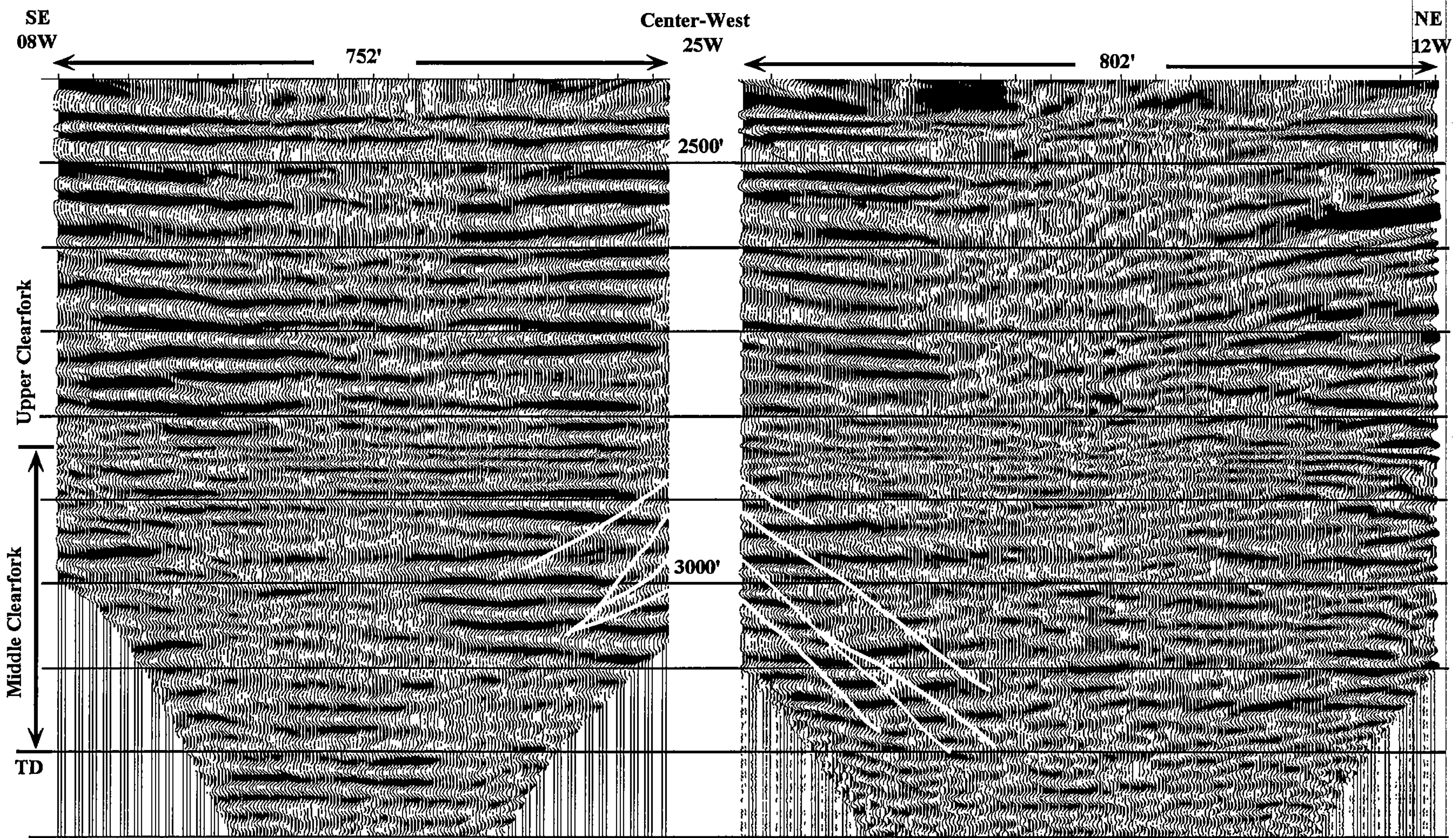

Figure 3. P-wave reflection images for two profiles around a central water injector. We have speculated on the existence of some faults near this injector that are within the reservoir zone. They are indicated by the white lines.

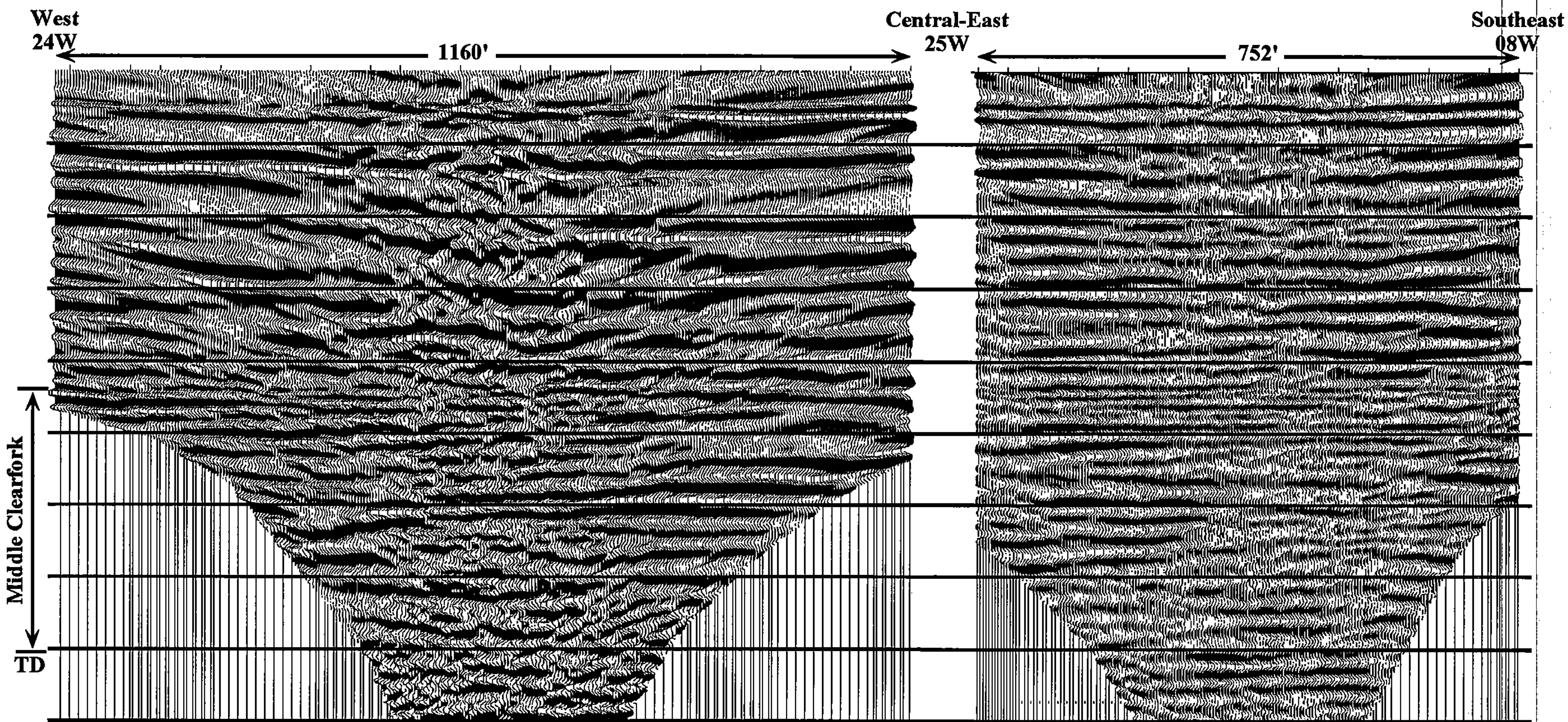

Figure 4. The east-west line on the left has the greatest well spacing (1160' nominal distance) and the poorest resolution. Therefore, we have not interpreted it. The profile on the right is from the previous figure, but flipped from left to right in order to make the tie at the well.

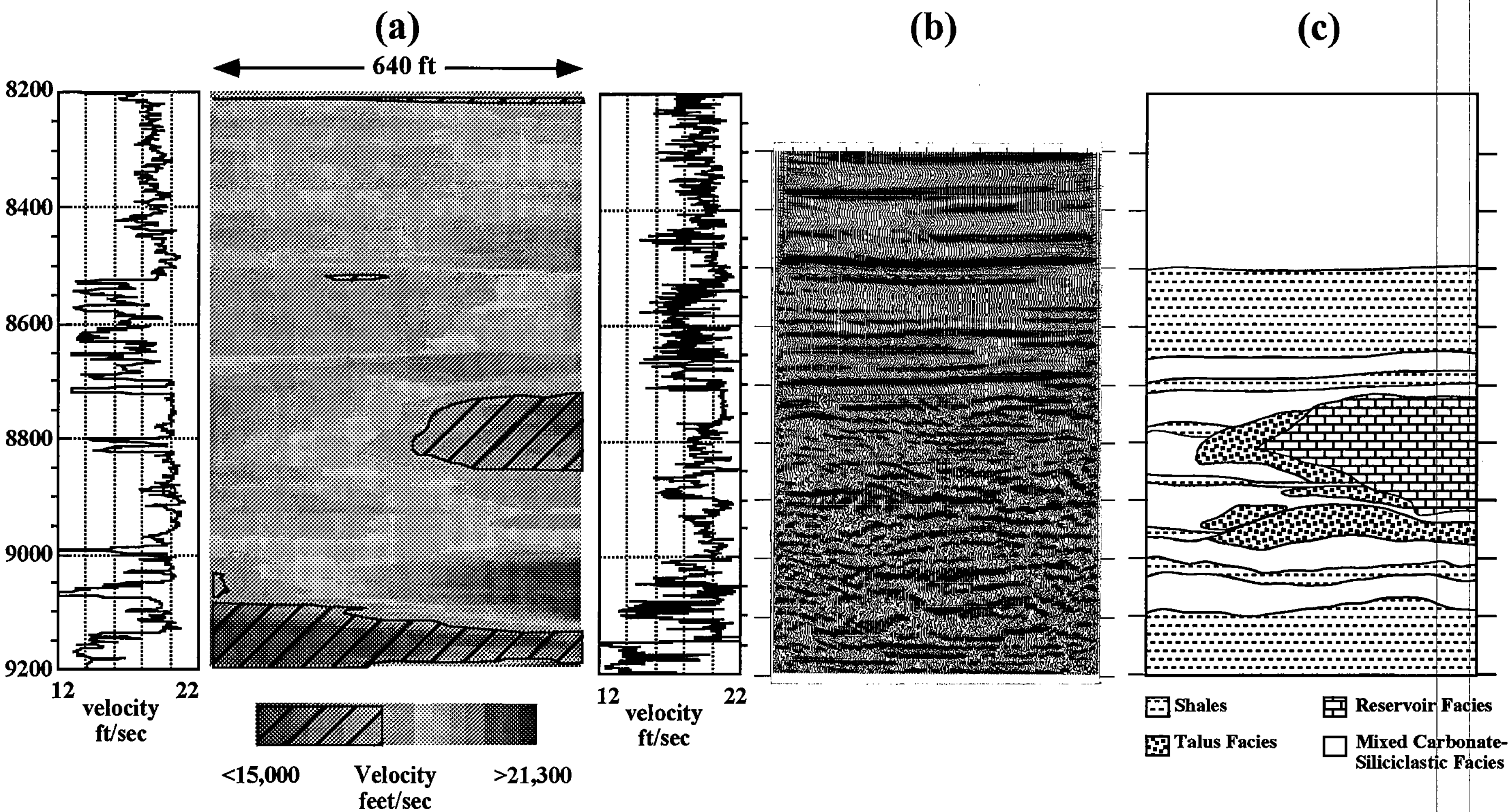

Figure 5. A crosswell tomographic velocity image, crosswell reflection image, and subsequent interpretation of the data associated with subtle anomalies present in surface seismic data.

Formulation of the inversion problem in terms of node-type models provides the capability to use adaptive gridding to address the problems of non-uniform ray coverage and inhomogeneous resolution. The spacing and density of nodes are adaptively selected to provide more uniform ray density per node or to match the geometrical pattern of the geological structure being imaged. In this way, reconstruction artifacts may be reduced, while velocity estimates are made more reliably. Also, "unknowns" are not wasted on homogeneous zones, but may be concentrated in heterogeneous regions of the image. Values of velocity at any point can be derived by interpolating the values at nearby nodes.

We have shown the sonic logs from each of the wells along the side of the tomogram. The anomaly from the surface data corresponds to the region between 8700 ft in depth and 9000 ft in depth in Well B.

The tomogram delineates an oval-shaped, low velocity zone extending from Well B to about the midpoint between the wells. Lower velocities in these carbonates often correlate with higher porosities. The corresponding crosswell reflection image, shown in Figure 5b, shows flat-lying internal structure or stratigraphy within this low velocity zone, and relatively flat-lying structure externally and to the left, but with some discontinuity in strata across the boundary. Below the low velocity region and between about 8900 ft and 8850 ft in depth are two small features about 300 ft apart. They consist of curved and dipping reflections, but with some flat-lying events in between.

This reflection image was obtained using the current wavefield separation and time-to-depth mapping methodologies of TomoSeis. An earlier generation of processing (circa early 1993) contained considerable tube wave energy and poorer bedding continuity, but the reflections we could see are consistent with the image presented here.

An interpretation of the reflection image, which incorporates knowledge obtained from the tomogram, the well logs, and core from Well B, is shown in Figure 5c. The reservoir facies is characterized by discontinuous reflections and low interval velocities, the talus facies by more continuous reflections and intermediate interval velocities, and the mixed carbonate-silicilastic facies by continuous events and fast interval velocities. The data suggest that the reservoir facies in Well B grade laterally into the talus facies, and then into the mixed carbonate-siliciclastic facies found in Well A.

CONCLUSIONS

Crosswell seismology is similar to other seismic techniques in that it includes both velocity estimation (i.e., tomographic imaging) and reflection imaging (i.e., VSP-CDP mapping and migration). Reflection imaging provides more resolution and is finding applications in reservoir delineation and characterization.

These images fill a resolution "gap" between surface seismic data and well log data. The surface seismic data can have a great deal of volumetric coverage of a reservoir, but have relatively poor resolution. Well log and core data have a high degree of resolution, but relatively poor volumetric coverage. One of our hopes for crosswell imaging is that by filling this resolution "gap", it will help us tie together the wide range of more traditional data types, while giving us an understanding of reservoir behavior at a unique scale of resolution.

Crosswell reflection imaging is in its infancy. The first reflection image obtained from data collected in the Permian Basin of West Texas dates back to only 1992 and significant strides have since been made in the imaging technology. The images shown in this paper are likely to change as they benefit from improvements in processing.

The interpretation of some of the features we see in these reflection images is speculative because of our limited experience with them. However, clearly it is unlikely we could obtain these subtle features from more traditional data types such as 3-D surface seismic data or well logs.

More powerful sources with greater bandwidths have been deployed since we collected the data in these case histories. These tools should result in higher quality data sets and greater well spacings then we have shown. In addition, multiple hydrophone strings are now being used to collect several profiles simultaneously, which has reduced acquisition costs.

ACKNOWLEDGMENTS

We would like to thank the Gas Research Institute for its financial support of the waterflood project, without which we would have been able to take the risk of acquiring the data over greater distances than were considered "safe" in 1993.

REFERENCES

Harris, J.M., 1994, An approach to adaptive gridding for traveltime tomography: Annual Report, Seismic Tomography Project, Stanford University.

Harris, J.M., Nolen-Hoeksema, R.C., Langan, R.T., Van Schaack, M.A., Lazaratos, S.K., and Rector, J.W., 1995, High-resolution crosswell imaging of a west Texas carbonate reservoir: Part 1-Project summary and interpretation, *Geophysics*, **60**, 667-681.

Harris, P.M., and Walker, S.D., 1988, McElroy Field, Central Basin Platform, U.S. Permian Basin, *in* Petroleum Geologists Treatise of Petroleum Geology: Atlas of Oil and Gas Fields, No. 1, Beaumont, E.A., and Foster, N. H., (ed.), 32 p.

Lazaratos, S.K., Harris, J.M., Rector, J.W., and Van Schaack, M.A., 1995, High-resolution crosswell imaging of a west Texas carbonate reservoir: Part 4-Reflection imaging, *Geophysics*, **60**, 702-711.

Ward, R.F., Kendall, C.G.ST.C., and Harris, P.M., 1986, Upper Permian (Guadalupian) facies and their association with hydrocarbons-Permian Basin, west Texas and New Mexico, *Am. Assoc. Petrol. Geol. Bull.*, **70**, 239-262.